2nd International Conference on System-Integrated Intelligence: Challenges for Product and Production Engineering

Changes of subsurface properties due to fatigue determined by sin²ψ-method and harmonic analysis of eddy current signals

B. Denkena[a], B. Breidenstein[a], W. Reimche[b], G. Mroz[b], T. Mörke[a]*, H. J. Maier[b]

[a]Institute of Production Engineering and Machine Tools, Leibniz Universität Hannover, An der Universität 2, 30823 Garbsen, Germany
[b]Institut für Werkstoffkunde (Material Science), Leibniz Universität Hannover, An der Universität 2, 30823 Garbsen, Germany

Abstract

Monitoring residual stress relaxation due to mechanical loading has the capability to retrieve a component's load history. So far, these changes are determined by X-ray diffraction using the sin²ψ-method going along with high effort regarding specimen preparation, measurement time and costs. The presented paper evaluates harmonic analysis of eddy current measurements as an alternative technology to determine alterations of a component's subsurface due to fatigue. Transferring this approach to a wide range of machined components and mass production bears the potential to gain access to large databases of service life information, representing an important enabling technology for cyber-physical systems.

1. Introduction

The Collaborative Research Centre SFB 653 "Gentelligent Components in Their Lifecycle" researches technologies enabling components to store information on their own production and to self-monitor their condition [1, 2]. The vision includes sensing components that communicate their load history. Future mass production components giving feedback based on real life application represent an invaluable knowledge for design evolution

---

* Corresponding author. Tel.: +49-511-762-4839; fax: +49-511-762-5115.
E-mail address: moerke@ifw.uni-hannover.de

regarding tailored adaptation to load. The current component condition and its load history can be used for maintenance and replacement. One key aspect is the possibility to determine whether and how a component has been loaded during the last maintenance interval and to estimate its failure possibility. Correlating the subsurface properties of a component during its lifecycle and its initial subsurface condition offers the possibility to determine its load history due to effects such as residual stress relaxation, change of dislocation density or work hardening. Therefore, the subsurface of machined components possesses high potential to enable the vision described above. At present, this information is not accessible in a simple way, and thus it has not been considered with regards to quality aspects. To access this information, current production process definition has to be extended beyond ordinary criteria such as productivity, components dimensions and surface quality.

In 1951 Henriksen investigated the surface integrity characteristics of components through an analysis of residual stress induced in machining processes [3]. The term surface integrity and typical surface characteristics such as plastic deformation, micro cracking and residual stress distribution were acknowledged by Field and Kahles [4]. Today's definition of residual stresses has been published by [5] in 1973. One of the most common approaches is the measurement of residual stresses in the near surface area by X-ray diffraction (XRD) and the $\sin^2\psi$-method [6]. As a result, residual stresses of the 1st order can be measured quantitatively, whereas 2nd order residual stresses are represented by the peak width at half maximum (FWHM) and have to be regarded as a qualitative indicator. The surface integrity and therefore the residual stress profile is an important attribute of a machined component, since it directly effects its fatigue life and fracture behaviour. The highest stress is located at the part's surface. Besides geometric irregularities, metallurgical alterations of the surface layer were identified to be important aspects of a surface regarding crack initiation. It could be demonstrated that compressive residual stress at a component's surface increases its fatigue life [7]. Nevertheless, the correlation of residual stress and functional performance needs to be understood in order to improve the performance and reliability of machined components [8]. The general influence of stress amplitude and number of cycles has been investigated extensively for different materials and heat treatment conditions. Experiments on AISI 4041 show an increasing residual stress relaxation for increasing load stress amplitude. It is demonstrated that the strongest relaxation appears for the first load cycles. The materials ultimate strength determines the residual stress sensitivity, which describes the degree of relaxation [9, 10, 11]. Various methods regarding the critical stress, which leads to residual stress relaxation, can be found in literature. Some approaches solely consider the load stress amplitude others include the residuals stress state prior to loading or the equivalent stress in the component based on the von Mises approach [9]. The majority in literature holds local plastic deformation following the shell/core approach [12] responsible for residual stress relaxation.

In addition to X-ray diffraction, eddy current measurement have been successfully applied for residual stress measurement [13]. The harmonic analysis utilises the superposition of an electromagnetic field caused by an exciting coil and a contrary aligned secondary electromagnetic field generated by eddy currents in the specimen and occurring magnetic reversal [14]. Changes in phase and amplitude of the 1st, 3rd and 5th harmonic response represent changes of the electrical and magnetic properties of the material, which are effected by residual stresses. Thus, eddy current measurement represents a fast and robust way of characterising material properties. Compared to X-ray diffraction it can be applied at large scale components without disassembling. Furthermore it requires less protective measures for staff and represents a smaller investment.

The presented work includes the characterisation of the specimen material as well as experimental results on subsurface properties after turning determined by X-ray diffraction and eddy current measurements. The response of the subsurface to fatigue experiments with an increasing load amplitude is analysed. Concluding, the results of X-ray diffraction and eddy current measurements are correlated.

2. Experimental setup

2.1. Preparation of specimens and characterisation of initial condition

Specimens for cyclic fatigue tests were machined on a Gildemeister CTX 520 L CNC lathe following DIN standard 50113 (smallest diameter 7 mm). The specimens' material was AISI 1060 high carbon steel in the as received condition. Yield and ultimate strength as well as yield point for compressive load and compressive strength of the material were experimentally determined (see fig. 1).
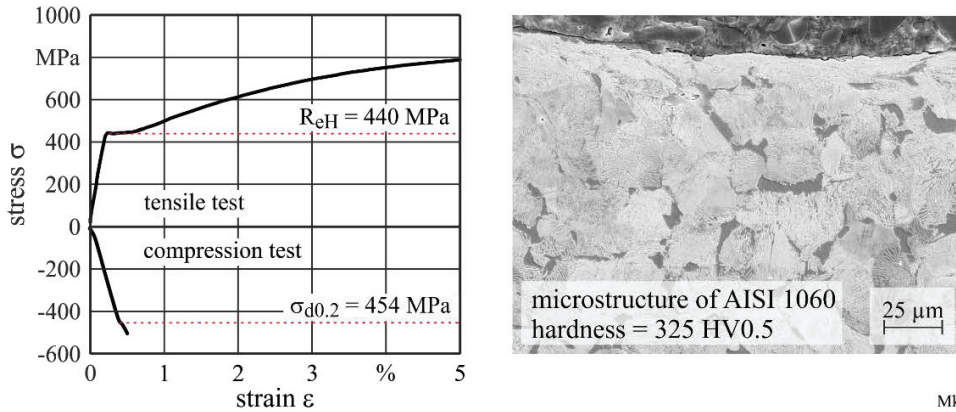
Fig. 1. Material properties of AISI 1060.

Following results of a previous publication [15], the cutting as well as tool parameters summarised in table 1 have been applied. Each specimen was machined using a new cutting edge to exclude the influence of wear. Due to a length of cut of $l_{c,max} = 350$ m, the effects of wear are not taken into account. The parameters are chosen to realise three types of specimen. Regarding the residual stresses in load direction, high tensile and compressive stresses due to varying passive forces as well as low and high cutting temperatures, are produced (fig. 4). These condition were evaluated by X-ray diffraction and $\sin^2\psi$-method regarding normal and shear stresses respective von Mises stress as well as peak width (FWHM). A point collimator with a diameter of 2 mm and CrKα radiation was employed causing a penetration depth of about 5 µm in steel [16]. The results are therefore integral measures of the residual stresses. 1st, 3rd and 5th harmonic response of eddy current excitation were correlated to identify an alternative method of qualitatively determine changes due to load in a shop floor environment.

Table 1. Process parameters and tool geometry.

process parameter		tool geometry: SNMA-120408-S02020-MW			
depth of cut	$a_p = 0.1$ mm	tool cutting edge angle	$\kappa_r = 75°$	tool orthogonal clearance angle	$\alpha_O = 5°$
cutting speed	$v_c = 30, 120, 300$ m/min	tool cutting edge inclination	$\lambda_S = -5°$	tool orthogonal rake angle	$\gamma_O = -5°$
feed rate	$f = 0.01, 0.1, 0.5$ mm	rounded cutting edge radius	$r_\beta = 50$ µm	corner radius	$r_\varepsilon = 0.8$ mm

X-ray diffraction and $\sin^2$-ψ method

Assuming plane stress in the near surface area the tensor S, which describes the residual stresses of the 1st order, is reduced from the general approach to the two dimensional equation (1).

$$S = \begin{bmatrix} \sigma_{xx} & \tau_{xy} & \tau_{xz} \\ \tau_{yx} & \sigma_{yy} & \tau_{yz} \\ \tau_{zx} & \tau_{zy} & \sigma_{zz} \end{bmatrix} \text{ simplified to } S = \begin{bmatrix} \sigma_{xx} & \tau_{xy} \\ \tau_{yx} & \sigma_{yy} \end{bmatrix} \text{ while } \tau_{xy} = -\tau_{yx}. \tag{1}$$

The residual stress measurements were carried out in $\xi = 0°$, 45° and 90° to the axial axis of the specimen representing σ_{xx}, σ_{yy} and σ_{xy}. Fig. 2 illustrates the location and orientation of the mentioned stresses [17].
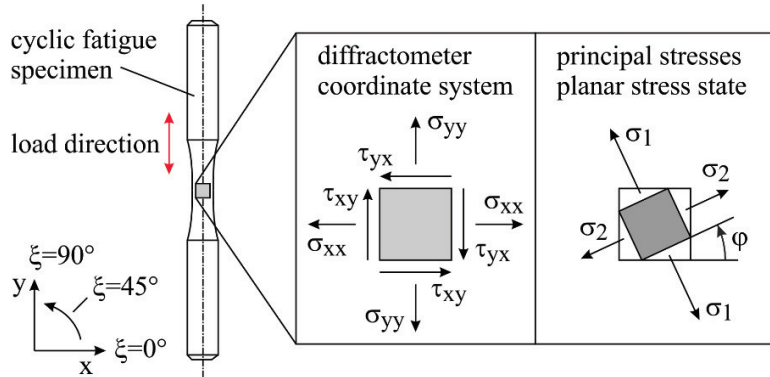
Fig. 2. Location and orientation of normal and shear stresses.

To determine the angle φ, which describes the rotation between the normal stresses coordinate system of σ_{xx} and σ_{yy} and the orientation of the principle stresses σ_1 and σ_2, which is defined by $\tau_{xy} = 0$, equation (2) was applied.

$$\varphi = \frac{1}{2}\tan^{-1}\left(\frac{\sigma_{xx} + \sigma_{yy} - 2\sigma_{xy}}{\sigma_{xx} - \sigma_{yy}}\right) \tag{2}$$

Equation (3) was used to determine the shear stresses τ_{xy} in the specimen coordinate system.

$$\tau_{xy} = \frac{\tan(2\varphi)\cdot(\sigma_{xx} - \sigma_{yy})}{2} \text{ and } \tau_{max} = \pm\frac{1}{2}(\sigma_1 - \sigma_2) \tag{3}$$

The residual stresses of the 1st order in the near surface area were determined to a full degree and can be expressed in the Mohr's circle. Fig. 3 illustrates the initial stress states induced by turning for the three different specimen types.
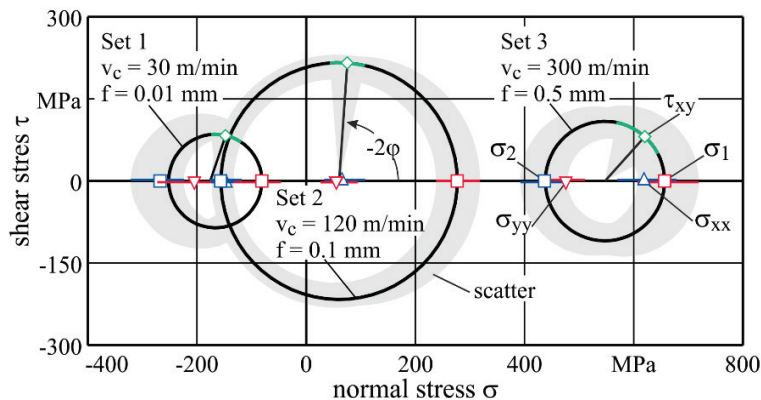
Fig. 3. Residual stress conditions visualised by Mohr's circle.

Its abscissa and ordinate represent normal and shear stresses respectively. The principle stresses σ_1 and σ_2 are used to draw a circle, which describes all possible normal and shear stress combination for a volume element cut under the rotation angle φ. The solid lines and marker represent the mean values of at least 16 individual specimens whereas the grey shading indicates the deviation. The corresponding values are listed in table 2.

Table 2. Summary of initial residual stresses and FWHM values in near surface area of specimens.

machining parameter			residual stresses								type II & III		surface hardness
			type I										
cutting speed (m/min)	feed (mm)	no. of samples	σ_{xx} (MPa)		σ_{yy} (MPa)		τ_{xy}* (MPa)		σ_v** (MPa)		FWHM (°)		HV 0.5
v_c	f	n	μ	s	μ	s	μ	s	μ	s	μ	s	-
30	0.01	19	-145	15	-205	35	-86	15	238	27	2.49	0.06	288
120	0.1	16	65	20	55	20	-216	13	381	24	2.57	0.02	300
300	0.5	21	620	35	475	25	-80	25	581	29	3.16	0.06	308
μ = mean value, s = std. dev. (sample), n = no. of samples, * following equation (3), ** following equation(4)													

The three different sets of specimen are located in a fully compressive, fully tensile and an intermediate condition. Especially the latter condition demonstrates the need to determine the full stress tensor, since the knowledge of just σ_{xx} and σ_{yy} (65 and 55 MPa) gives the impression of fully tensile stresses at the specimens' surface. Rotating the direction of an applied load stress visualises that due to the high shear stress, significant compressive or tensile stresses counteract. Since the residual stress condition in the near surface area in the specimens' coordinate system does not match the principal stresses, the shear stresses have to be considered to describe the effective stress, when the load is applied. The full knowledge of the stress tensor enables the determination of the equivalent stress σ_v following equation (4) by von Mises [18] to compare the stress condition. In order to describe the influence of fatigue on the stress tensor S the relaxation is expressed by means of σ_v and correlated to the load stress amplitude.

$$\sigma_v = \sqrt{\sigma_{xx}^2 - \sigma_{xx} \cdot \sigma_{yy} + \sigma_{yy}^2 + 3 \cdot \tau_{xy}^2} \tag{4}$$

To qualitatively determine 2nd order residual stresses, the width of the X-ray peak at its half maximum was considered. As described earlier, three measurements of each specimen were carried out, therefore the values for FWHM given in table 2 are the mean values measurements at $\xi = 0°$, 45° and 90°. The increasing equivalent stress is directly accompanied by an increasing mean value of FWHM. As a possible cause the mechanical inducement of dislocations is assumed. This is confirmed by an according increment of the surface hardness (table 2). It is noted that various material properties e.g. chemical composition, phases, grain size and refinement, have significant influence on the absolute value of FWHM. The latter can be influenced by machining. Therefore the relative change rather than the absolute value is considered regarding the qualitative description of subsurface changes respectively 2nd order residual stresses.

Harmonic analysis of eddy current signals

The mechanical as well as the electromagnetic material characteristics are determined by the alloy composition, the crystalline structure, grain size and the materials strain. In ferromagnetic materials eddy current signal depend on the characteristics of the magnetic hysteresis. Because of the nonlinear dependency of magnetisation and magnetic field higher harmonics of the measuring frequency are caused, which are characteristic for the state of the material [14]. Mechanical and electrical properties of each specimen are determined by the 1st, 3rd and 5th harmonic. The 3rd and 5th harmonic response are regarded to qualitatively give information on residual stresses [13]. Details on the experimental setup are summarised in table 3. Due to the skin-effect, the penetration depth δ of the presented method is limited, and therefore, it is vital for the interpretation of the results. It is estimated following equation (5) [19]:

$$\delta = \sqrt{\frac{1}{\pi \cdot f_p \cdot \sigma_{elec} \cdot \mu_0 \cdot \mu_r}} \qquad (5)$$

Table 3. Details of eddy current measurement.

probe diameter d (mm)	core material	current I (A)	voltage U (V)	excitation frequency f_p (kHz)
12	ferrite	0.6	4	3.2

The penetration depth is defined as the distance from the specimen's surface where the eddy current density drops to 1/e (approximately 36.8 %) as compared to the value at the surface. Besides the experimentally determined electrical conductivity $\sigma_{elec} = 7.9$ 1/(Ωm) the magnetic permeability μ_r has to be determined. Based on measurements for AISI 1035 low carbon steel a bandwidth of $\mu_r = 400 \pm 200$ was taken into account. Accuracy can be increased with specific measurement of μ_r. Since it changes depending on the magnetic field strength, a bandwidth similar to AISI 1035 is expected. Following equation (5), applying the vacuum permeability, $\mu_0 = 4 \cdot \pi \cdot 10^{-7}$ Vs/(Am), an excitation frequency of $f_p = 3.2$ kHz causes a penetration depth $\delta = 177 \pm 48$ µm. Fig. 4 illustrates the penetration depth of eddy current measurement and X-ray diffraction regarding the measured residual depth profiles of the specimens.
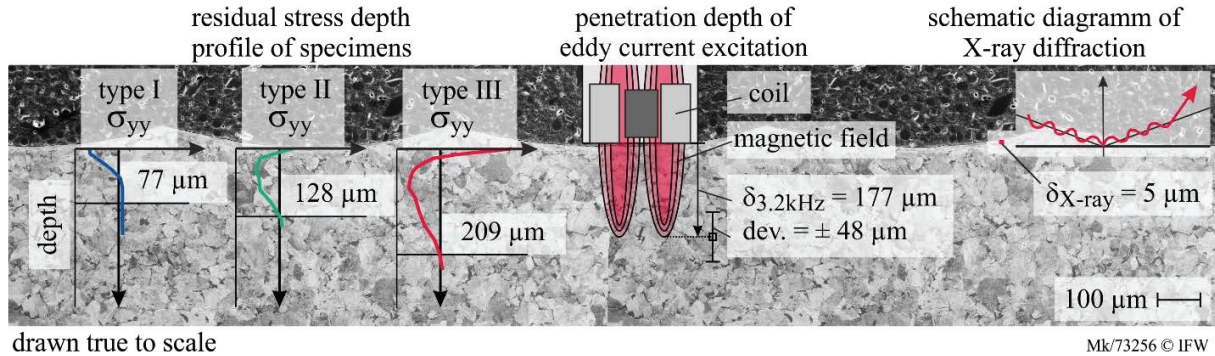

Fig. 4. Penetration depth of eddy current measurement and X-ray diffraction.

It can be demonstrated that the depth probed by eddy current is 62-290 % of the depth effect of residual stresses. Therefore, the reduction of the penetration depth leads to a better comparability of the two methods.

Table 4. Summary of 1st, 3rd and 5th harmonic response of eddy current excitation for initial specimen conditions.

machining parameter		amplitude of harmonic response			
cutting speed v_c (m/min)	feed f (mm)	1st harmonic response (mV)	3rd harmonic response (µV)	5th harmonic response (µV)	no. of samples n
30	0.01	1.125	14.813	1.507	8x6
120	0.1	1.157	13.531	1.225	8x6
300	0.5	1.102	12.688	1.331	8x6

The comparison of absolute numbers is prone to errors due to slight changes of the coupling conditions or the electric respective magnetic field. Therefore, relative values were used to describe changes of the surface and subsurface conditions due to mechanic load.

2.2. Alternating bending loads

The specimens were loaded with fully revered stress for 1000 cycles. To determine the critical stress amplitude depending in the residual stress condition, it is increase from $\sigma_{load} = 21\ \%\ R_m$ to 53 % R_m. At 45° and 225° along the circumference, the specimen experiences an alternating tensile-compressive stress. At 0° and 180° a neutral phase without stress results. The neutral phase is considered a comparison measurement, since no changes should occur. Since the residual stress condition in the coordinate system of the specimen do not match the principal stresses, the shear stresses have to be considered to describe the effective stress. Therefore, to determine the effective stress at the specimen's surface at the maximum stress, the von Mises equation is extended by σ_{load}. Due to the uniaxial load the effective von Mises stress is describes as:

$$\sigma_v^* = \sqrt{\sigma_{xx}^2 - \sigma_{xx} \cdot \left(\sigma_{yy} + \sigma_{load,yy}\right) + \left(\sigma_{yy} + \sigma_{load,yy}\right)^2 + 3 \cdot \tau_{xy}^2} \tag{6}$$

In the following, equation (6) is used to identify stress amplituds, which lead to exceedance of the static yield strength R_e of the material and therefore to local plastic deformation and residual stress relaxation in the near surface area.

3. Results and discussion

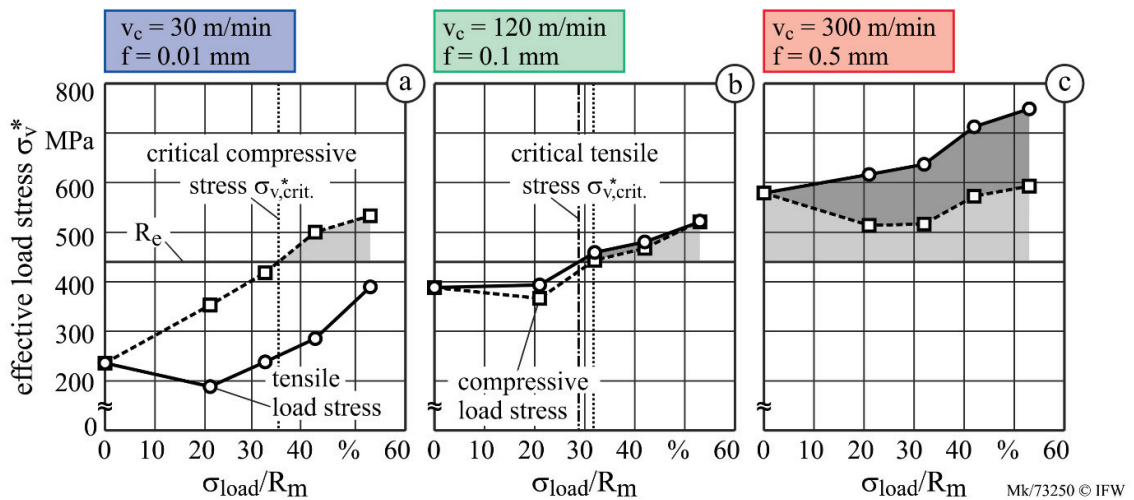### 3.1. Relaxation of 1st and 2nd order residual stresses

Fig. 5. Effective von Mises stress for compressive and tensile loads based on residual stresses prior to loading and maximal stress.

Experiments with increasing loads show that the residual stresses relax, if the sum of residual stress in the near surface area and the load stress amplitude exceed the yield strength of the material. Fig. 5 illustrates the effective von Mises stress σ_v^* based of residual and maximal stress amplitude (equation (6)). The stress amplitude is expressed depending on the material as ratio of the stress amplitude σ_{load} and the ultimate strength of the material R_m. Depending on the residual stress state, the yield strength R_e is exceeded either due to compressive or tensile stresses. The residual stress depth profile shown in fig. 4 illustrate that machining induced residual stresses effect just near surface areas. Therefore, exceedance of yield strength by the effective stress does not lead to a global component deformation, but residual stress relaxation by local material flow. Due to high compressive residual stresses induced by machining, specimens reach critical effective von Mises stresses $\sigma_{v,crit}^*$ when a compressive load $\sigma_{load} \approx 35\ \%\ R_m$ is applied (fig. 5-A). A compressive residual stress condition, reduces the effective stress due to tensile loads.

Specimens shown in fig. 5-C exceed the theoretical threshold without the application of additional stress, since a high amount of tensile stresses is induced by machining. Thus, the smallest load applied (σ_{load} = 20% R_m) is expected to cause residual stress relaxation.
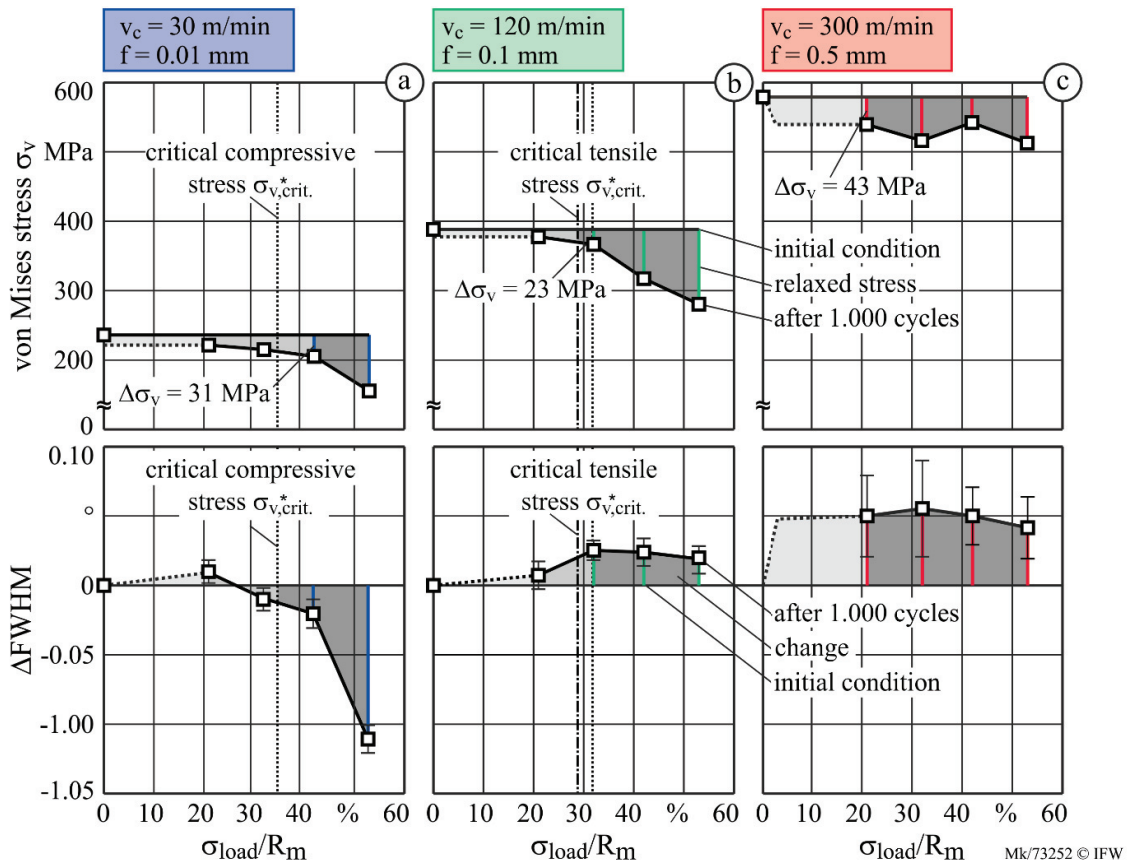

Fig. 6. Relaxation of 1st and 2nd order residual stress depending on ratio of stress amplitude and ultimate strength.

The residual stresses were measured after the fatigue tests and compared to the initial condition. The 1st and 2nd order residual stress relaxation is illustrated in fig. 6. The amount of equivalent stress relaxed increases with the stress amplitude, whereas the amount of relaxation cannot be correlated with a specific combination of stress amplitude and number of load cycles, yet. At first, the amount of relaxed stresses for the identified critical stresses ($\Delta\sigma_v$ = 31 MPa, 23 MPa and 43 MPa) appears rather small as compared to the standard measurement error of the $\sin^2\psi$-method (about ±20 MPa). Hence, it is pointed out that the residual stresses show relaxation with higher significance for single tensor components. This is due to the structure of the von Mises equation. The local plastic deformation initiated by effective von Mises stresses above R_e also lead to changes of the FWHM, indicating changes of 2nd order residual stresses. For specimens with initially high equivalent stress due to tensile stresses, all load amplitudes show similar changes. It is pointed out that this specific specimen type also shows high scatter. The behaviour of FWHM corresponds to the results for the 1st order residual stress relaxation. Since it is rather small as compared to the accuracy of the X-ray diffraction, this correlation can be used to increase the methods significance.

3.2. Change of 5th harmonic response of eddy current measurement

The presented X-ray diffraction results can be correlated with the changes of the 5th harmonic response of the eddy current measurement. Fig. 7 illustrates the amplitude changes for eddy current analyses along the

circumference of the specimens. This was carried out for all specimen types and stress amplitudes. Each diagram illustrates the measurement prior and after the stress was applied. The change of phase was also analysed, but data is not shown here for the sake of brevity. At 0° and 180° along the circumference, the neutral phase of stress is located. For specimen type I (residual stresses in load direction $\sigma_{yy} = -145$ MPa), critical load is exceeded for $\sigma_{load} > 35$ % R_m. 1st order residual stresses show changes of $\Delta\sigma_v = 31$ MPa for $\sigma_{load} = 42$ % R_m at which the 5th amplitude of harmonic response shows significant changes. The change increases with the stress amplitude. The two peaks along the circumference can explicitly associated to the maximal and neutral stress phase.
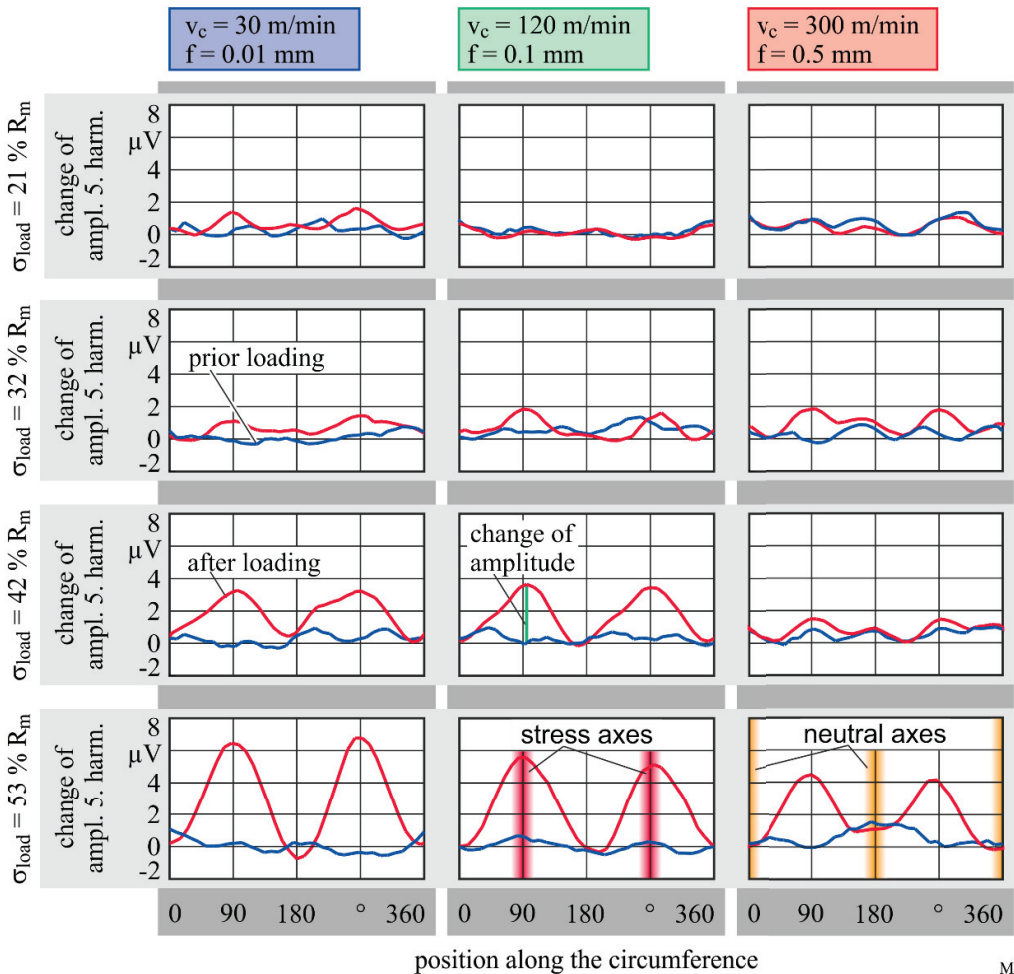

Fig. 7. Change of amplitude of 5th harmonic response amplitude and phase.

For high stress amplitudes ($\sigma_{load} > 32$ R_m) changes of the 5th harmonic amplitude can be determined for type II specimens (residual stresses in load direction $\sigma_{yy} = +65$ MPa). A significant change in phase but weak in amplitude can be determined for $\sigma_{load} = 32$ % R_m. In this case $\sigma^*_{v,crit} \approx 30$ % R_m is slightly exceeded regarding tensile stress. Eddy current analyses of specimen type III (residual stresses in load direction $\sigma_{yy} = +620$ MPa), which shows strong 1st and 2nd order residual stress relaxation present higher significant changes. This effect might be related to a higher tendency of crack initiation rather than local plastic flow due to tensile stress exceedance. The effect is not jet explained and is subject of further investigations. Current research also focuses on a reduction of the penetration depth of eddy current to focus on the near surface area effected by residual stresses. Following equation (5) a

B. Denkena et al. / Procedia Technology 15 (2014) 503 – 513

doubling of the frequency to e.g. $f_p = 6.4$ kHz decreases the penetration depth to $\delta = 125\pm34$ μm, which represents 44-205 % of the depth, effected by residual stresses.

4. Conclusion

The presented study focused on the characterisation of subsurface properties after turning. The response of the subsurface to fatigue experiments with an increasing load stress amplitude was analysed by X-ray diffraction and eddy current measurements. It could be demonstrated that the residual stress relaxation in the near surface area correlates with the 5th harmonic analyses by means of phase and amplitude. The results can be summarised as follows:

- residual stresses relax depending on the ratio of stress amplitude and ultimate strength of the material
- based on residual stress initial condition the critical load stress $\sigma^*_{v,crit}$ can be determined by the von Mises hypotheses and stress amplitude (see equation (6))
- eddy current measurements show promising results when compared to X-ray diffraction data and thus, may be qualified as an alternative method regarding shop floor application
- reduction of eddy current penetration depth is expected to increase the correlation quality
- The exceedance of the effective equivalent stress due to compressive stress appears to cause a change of phase and amplitude of the 5th harmonic analyses of the eddy current measurement whereas tensile stress exceedance show stronger influence on the phase than the amplitude.

Acknowledgements

References

[1] Denkena B, Henning H, Lorenzen LE. Genetics and intelligence: New approaches in production engineering. Prod. Eng. 2010;4:65–73.
[2] Denkena B, Mörke T, Krüger M, et al. Development and first applications of gentelligent comp. over their lifecycle. JMST 2014;7(2):139-150.
[3] Henriksen EK. Residual stresses in machined surfaces. Transactions of the ASME 1951;73:69–74.
[4] Field M, Kahles JF. The surface integrity of machined and ground high strength steels. DMIC Report 1964;210:54-77.
[5] Macherauch E, Wohlfahrt U, Wolfstieg. Zur zweckmäßigen Definition von Eigenspannungen. Härterei-Tech. Mitt. 1973;28:201-211.
[6] Macherauch E, Müller P. Das $\sin^2\psi$-Verfahren der röntgenographischen Spannungsmessung. Z. für Angewandte Physik 1961;13:305–312.
[7] Withers PJ. Residual stress and its role in failure. Reports on Progress in Physics 2007;70(12):2211–2264.
[8] M'Saoubi R, Outeiro JC, Chandrasekaran H, Dillon Jr OW, Jawahir IS. A review of surface integrity in machining and its impact on functional performance and life of machined products. IJSM 2008;1(1–2):203–236.
[9] Macherauch E, Wohlfahrt H. Eigenspannungen und Ermüdung. In: Ermüdungsverhalten metallischer Werkstoffe. DGM-Informationsgesellschaft Verlag 1985:237-283.
[10] Scholtes B. Eigenspannungen in mechanisch randschichtverformten Werkstoffzuständen, Ursachen-Ermittlung-Bewertung. 1st ed. Oberursel: DGM-Informationsgesellschaft; 1990
[11] Schulze V. Modern mechanical surface treatment. States, stability, effects. 1st ed. Weinheim: Wiley-Verlag; 2006
[12] Vöhringer O, Wohlfahrt H. Abbau von Eigenspannungen. In: Hauk V, Macherauch E, editors. Eigenspannungen und Lastspannungen, Moderne Ermittlung, Ergebnisse, Bewertung. München: Carl Hanser Verlag; 1982. p. 49-83
[13] Stroppe H, Schiebold K. Wirbelstrom – Materialprüfung. 1st ed. Wuppertal: Castell Verlag; 2005.
[14] Heutling B. Zerstörungsfreie Online-Materialcharakterisierung von Stahlfeinblechen mittels Harmonischen Analyse von Wirbelstromsignalen. PhD thesis, Leibniz Universität Hannover; 2004.
[15] Denkena B, Köhler J, Breidenstein B, Mörke T. Elementary studies on the inducement and relaxation of residual stress, Procedia Engineering 2011;19:88-93.
[16] Brinksmeier E. State of the Art Non Destructive Measurement of Subsurface Material Properties and Damages. Precision Engineering 1989;11:211-224.

[17] Dölle H, Hauk V. Röntgenographische Spannungsermittlung für Eigenspannungssysteme allgemeiner Orientierung. Härterei-Tech. Mitt. 1976;31:165-168.

[18] von Mises R. Mechanik der festen Körper im plastisch deformablen Zustand. Göttin. Nachr. Math. Phys. 1913;1:582–592.

[19] EN ISO 15549:2010. Non-destructive testing - Eddy current testing - General principles. 2010.